



Control of the gastrointestinal digestion of solid lipid nanoparticles using PEGylated emulsifiers



Choongjin Ban^{a,1}, Myeongsu Jo^{b,1}, Seokwon Lim^d, Young Jin Choi^{a,b,c,*}

^aCenter for Food and Bioconvergence, Seoul National University, 1 Gwanakro, Gwanakgu, Seoul 08826, South Korea

^bDepartment of Agricultural Biotechnology, Seoul National University, 1 Gwanakro, Gwanakgu, Seoul 08826, South Korea

^cResearch Institute of Agriculture and Life Sciences, Seoul National University, 1 Gwanakro, Gwanakgu, Seoul 08826, South Korea

^dDepartment of Food and Biotechnology, Hoseo University, 79-20 Hoseoro, Asan, Chungnam 336-795, South Korea

ARTICLE INFO

Article history:

Received 1 February 2017

Received in revised form 22 May 2017

Accepted 26 June 2017

Available online 27 June 2017

Keywords:

Solid lipid nanoparticle

Polyethylene glycol

Oral administration

Gastrointestinal digestion

Controllable digestion

ABSTRACT

We prepared solid lipid nanoparticles (SLNs) with tristearin and various emulsifiers which had different chain length PEGs (10–100 times-repetition of ethylene glycol) to control their digestion fate in the gastrointestinal tract. Fabricated SLNs after acidic/high-ionic-strength media treatment were stable regardless of the ζ -potential (ZP) disappearance. Additionally, highly PEGylated SLNs successfully hindered the adsorption of both bile acid (BA) and lipase on the SLN surface, while lowly PEGylated SLNs interrupted that of only lipase. In simulated small intestinal fluid, lipolysis of highly PEGylated SLNs increased with decrease of the emulsifier density on the SLNs, whereas lipolysis of lowly PEGylated SLNs increased with decrease of the particle size. These results suggested that high PEGylation was more efficient than low PEGylation to hinder the lipolysis initiated from the competitive replacement of the SLN-covering emulsifiers with BAs. Consequently, the SLN digestion could be controlled by choosing the length and concentration of PEGylated emulsifiers.

© 2017 Elsevier Ltd. All rights reserved.

1. Introduction

Controllable digestion of a lipid carrier system in the gastrointestinal tract (GIT) is a large issue that needs to be solved to successfully develop functional foods that are fortified to increase biological activities, as digestion effects the bioavailability and controlled release of bioactive materials incorporated into carriers (McClements, Decker, & Park, 2008; Porter, Pouton, Cuine, & Charman, 2008). Ingested lipid carrier systems should travel from the mouth to intestine along the lumen and experience various environmental changes, e.g., mouth: neutral pH, high ionic strength, mucin, amylase, lingual lipase and so on; stomach: low pH, high ionic strength, mucin, pepsin, gastric lipase and so on; and small intestine: neutral pH, high ionic strength, pancreatic lipase, colipase, bile salts and phospholipids (Kong & Singh, 2008; McClements & Xiao, 2012). During the retention time in the GIT, the acidic conditions in the stomach could bring the unwanted aggregation of the carriers, and lingual, gastric, or pancreatic lipase could hydrolyze the lipid molecules in the carriers. Particularly,

lipid digestion occurs mainly in the small intestine (70–90%) by pancreatic lipases with the help of calcium ions, bile salts and colipase (Maldonado-Valderrama, Wilde, Macierzanka, & Mackie, 2011). Therefore, the controllable digestion of the lipid carriers can be accomplished by preventing the collision among the lipid droplets and the action of various lipases, colipase, and bile salts at the lipid-water interface. In this regard, understanding this interface of lipid carrier systems would be a key point to modulate their GIT digestion.

Many researchers have strived to control the lipid hydrolysis by means of modulating the interfacial properties. Maldonado-Valderrama et al. examined the compositional changes of the β -lactoglobulin-stabilized lipid surface by ionic surfactants (Tween 20) and biological surfactants (bile salts) during the digestion process (Maldonado-Valderrama, Gunning, Ridout, Wilde, & Morris, 2009; Maldonado-Valderrama, Gunning, Wilde, & Morris, 2010; Maldonado-Valderrama et al., 2008). Chu et al. studied the interfacial changes induced by bile salts and the adsorption of colipase and pancreatic lipase onto the interface, and then suggested that galactolipids on the lipid surface could slow the rate and extent of lipid digestion in the GIT (Chu et al., 2009, 2010). Furthermore, the controllable digestion method of oil droplets under *in vitro* small intestinal conditions was introduced using a non-ionic emulsifier (Poloxamer 188) (Torcello-Gómez, Maldonado-Valderrama,

* Corresponding author at: Department of Agricultural Biotechnology, Seoul National University, 1 Gwanakro, Gwanakgu, Seoul 08826, South Korea.

E-mail address: choijy@snu.ac.kr (Y.J. Choi).

¹ These authors contributed equally to this work.

Martín-Rodríguez, & McClements, 2011). These literature examples are representative instances to demonstrate the possibility of controllable lipid digestion by modulating the design of the interfacial composition. However, it is still unclear what size and quantity of emulsifiers at the interface can effectively hinder the action of active components on the biological surface, such as bile salts, colipase and lipase.

The solid lipid nanoparticle (SLN) system has been regarded as an attractive lipid carrier system due to the use of solid-state lipid at room/body temperatures. The solid lipid in SLNs has some merits for delivering bioactive materials, i.e., a rigid matrix capable of protection from the outside and offering the possibility for the controlled release of the bioactive components (Müller, Mäder, & Gohla, 2000). Polyethylene glycol (PEG) is a synthetic polymer approved for its safety in the body (Nagaoka & Nakao, 1990), which has been universally used in pharmaceuticals and cosmetics, as well as in foods. PEGs with large chains above a certain level (~2 kDa) can sterically repel the approach of proteins, including enzymes, and have the ability to avoid detection by the immune system in the body (Jeong, Park, & Kim, 2011). In this manner, many molecules or macrostructures are covalently/non-covalently attached with PEGs to have a “stealth function” in the body, which is called as PEGylation (Gref et al., 2000; Niidome et al., 2006). Müller and coworkers achieved the modulation of the lipolysis of PEGylated SLNs under simulated GIT conditions using Poloxamer 188 (Müller, Rühl, & Runge, 1996) and Poloxamer 407/cholic acid (Olbrich & Müller, 1999). However, the colipase/lipase adsorption and surfactant displacement on the lipid surface were unclear. Therefore, the mechanisms of SLN digestion should be verified, along with considering the compositional changes of the interface at a molecular level.

In this study, SLNs prepared using tristearin (TS) and various PEGylated emulsifiers were utilized, and the number of emulsifiers participating in covering the SLN surface was quantitatively determined for consideration on a molecular level. Moreover, under the mimicked *in vitro* GIT environment, the digestion patterns of the PEGylated SLNs were monitored to determine the effects of the type/concentration of PEGylated emulsifier at the lipid-water interface on the SLN digestion, followed by the action of bile acids (BAs), colipase and pancreatic lipase. On the basis of the obtained results, we suggested the digestion mechanism of PEGylated SLNs on a molecular level, as well as the controllable hydrolysis methods of the SLNs.

2. Materials and methods

2.1. Chemicals

Glyceryl tristearate (tristearin), polyoxyethylene (10) stearyl ether (PEG10SE, Brij® S10), polyoxyethylene (100) stearyl ether (PEG100SE, Brij® S100), polyoxyethylene (10) oleyl ether (PEG10OE, Brij® O10), decaethylene glycol monododecyl ether (PEG10LE) and polyoxyethylene sorbitan monostearate (PEG20SS, Tween® 60) were purchased from the Sigma Aldrich Co. (St. Louis, MO, USA). Polyethylene (10) stearate (PEG10S) and polyoxyethylene (100) stearate (PEG100S, Myrj® S100) were obtained from TCI (Tokyo, Japan) and Croda (Parsippany, NJ, USA), respectively. All other chemicals were of analytical reagent grade.

2.2. Solid lipid nanoparticle preparation

The SLNs were prepared using an oil-in-water emulsion technique with a high-speed blender and sonication probe as suggested previously by our group (Ban, Lim, Chang, & Choi, 2014), with slight modifications. First, the lipid (5 wt%) and aqueous (95 wt%)

phases were heated to 95 °C and mixed using a high-speed blender (Ultra-Turrax T25D, Ika Werke GmbH & Co., Staufen, Germany) at 8,000 rpm for 1 min and then at 11,000 rpm for 1 min while being maintained at 95 °C. The lipid phase of the SLNs was composed of TS, while the aqueous phase was fabricated by adding PEGylated emulsifiers until reaching the pre-determined concentration (5.331, 17.058, 25.588, 34.117, or 46.910 mM of the entire SLN system) in double-distilled water (DDW) containing 0.02 wt% sodium azide with mixing for 1 h. After preparing the coarse oil-in-water emulsion, the droplet size was further reduced by sonication (VCX 750, Sonics & Materials Inc., Newtown, CT, USA) for 4 min at 60% amplitude, a duty cycle of 1 s, and 95 °C. After reducing the droplet size, post-sonication was applied for 6 min to the emulsions during cooling to 25 °C in a jacketed beaker, and the samples were maintained at room temperature (25 °C).

2.3. Quantifying non-aggregated solid lipid nanoparticles (yield %)

SLNs diluted 10-fold with DDW were passed through a 1 µm pore size glass microfiber filter (GF/B, Whatman Ltd., Loughborough, UK). The aggregated SLNs remaining on the filter (micron-scale) were weighed after drying in an oven at 50 °C. The difference in filter weight before and after the procedure, which was the weight of the creamed or aggregated SLNs, was recorded.

2.4. Measuring the solid lipid nanoparticle size and ζ-potential

The prepared SLNs (4.5 ml) were diluted with 40.5 ml of DDW in a vial to separate the layers containing the aggregated and non-aggregated SLNs. The vial containing the diluted samples was sealed tightly with a screw cap and incubated overnight at ambient temperature. The aggregated SLNs were removed by filtration with a 1 µm pore size glass microfiber filter (GF/B, Whatman Ltd.), and the mean size (z average) of the passed particles was measured using a Zetasizer (Nano ZS, Malvern Instruments Ltd., Worcestershire, UK) operated at a 173° angle with a helium-neon laser ($\lambda = 633$ nm). In addition, the ζ-potential (ZP) was also measured using the Zetasizer. The ZP measurement was based on the Smoluchowski equation at 25 °C with an electric field strength of 20 V cm⁻¹.

2.5. Determining the emulsifier surface load

Using an assumption of a spherical shape for all of the SLNs (Fig. S1 in Supplementary Material), the emulsifier surface load (Γ_s) was calculated as follows: $\Gamma_s = C_a D / 6 \Phi_v$, where C_a is the concentration of the emulsifier adsorbed onto the surfaces of SLNs, D is the mean diameter (z average), and Φ_v is the lipid phase volume fraction (i.e., 0.05 lipid phase) (McClements, 2007). C_a was measured by subtracting the concentration of emulsifiers suspended as single molecules or micelles from the initial concentration of total emulsifiers in the aqueous phase. A total of 2.5 ml of the previously diluted and filtered SLN dispersion system was injected into the Sephadex G-25 column (GE Healthcare, Chalfont St Giles, UK) filled with DDW. Next, 1 ml of DDW was serially added, and then each fraction passing through the column was collected in a micro-tube. Subsequently, aliquots of the fractions in the fifth and sixth tubes were selected as samples in which the emulsifier molecules did not participate in any emulsifying activity. Colorimetry for the quantification of PEGylated emulsifiers has been reported previously (Khossravi, Kao, Mrsny, & Sweeney, 2002). Briefly, each sample was dried at 60 °C in an oven. The sample was then cooled in ambient conditions, and 0.6 ml of ammonium cobaltothiocyanate (ACTC) solution as well as 1.2 ml of dichloromethane were added. The ACTC solution was prepared using 3 g of cobalt nitrate hexahydrate and 18 g of ammonium thiocyanate in 100 ml of DDW. Samples were vortexed for 10 s

and then centrifuged at 10,400 RCF for 10 min (5427R, Eppendorf AG, Hamburg, Germany). After centrifugation, the dichloromethane layer was transferred to a micro quartz cell, and the absorbance at 625 nm was determined using a spectrophotometer (Pharmaspec UV-1700, Shimadzu Corp., Kyoto, Japan). The quantity of emulsifier molecules in the samples was calculated using standard curves over the ranges of 15.625–1000, 6.25–375, 62.5–1000, 31.25–2000, 15.625–1000, 6.25–800, and 12.5–800 $\mu\text{g ml}^{-1}$ for PEG10S, PEG100S, PEG10SE, PEG100SE, PEG10OE, PEG10LE, and PEG20SS ($R^2 = 0.9970, 0.9406, 0.9998, 0.9970, 0.9998, 0.9997$, and 0.9998), respectively.

2.6. Measuring the size and ζ -potential of solid lipid nanoparticles after treatment with high ionic strength and acidic media

For monitoring the influence of various salts in the GIT and low pH in the stomach on the colloidal stability of the SLNs, the size and ZP of the particles were measured after incubating the SLNs in high ionic strength and acidic conditions. Prior to determining the stability of SLNs in these conditions, SLNs were diluted 10-fold, and then, the aggregated particles were eliminated by filtration (1 μm). To achieve high ionic strength conditions, 5 ml of the diluted and filtered SLNs was blended with 3.8 ml of the mixture of all media and juices except for the HCl solution, proteins, bile and enzymes in Table S1 (Supplementary Material) (Hur, Joo, Lim, Decker, & McClements, 2011), and then it was adjusted to a pH of 7 using 1 M NaOH or 1 M HCl solution with monitoring using a pH meter (Professional Meter PP-15, Sartorius AG, Goettingen, Germany). For the experiments under acidic conditions, the pH of the diluted and filtered SLN samples was adjusted to 3 using a 50 mM HCl solution with monitoring on a pH meter. After the treatment under high ionic strength and acidic conditions, samples were incubated in a shaking water bath (BS-31, JEIO Tech., Seoul, Korea) for 2 h at 37 °C with shaking (100 rpm). After the incubation, 2 ml of the samples was centrifuged for 10 min at 25,000 RCF to eliminate the poor reliability originating from the creamed SLN aggregates in subsequent measurements, and 1 ml of the supernatants was used to measure the size and ZP of the particles in the samples using the Zetasizer. The relative centrifugal force (25,000 RCF) applied for the centrifugation was predetermined based on preparatory experiments, which did not induce the creaming and sedimentation of freshly prepared SLNs after the centrifugation treatment.

2.7. Measuring the size and ζ -potential of solid lipid nanoparticles after treatment with pancreatic lipase and bile extract

To assess the effects of digestive enzymes, bile and proteins secreted in the small intestine on the characteristics of SLNs, the size and ZP of the particles were measured after treatment with pancreatic lipase or bile extract solution. Five milliliters of SLNs previously diluted (10-fold) and filtered (1 μm) was treated with pancreatic lipase (3.965 mg ml^{-1}) or bile extract (41.32 mg ml^{-1}) solution at pH 7, adjusted to a pH of 7 using 1 M NaOH or 1 M HCl solution, and then incubated for 2 h at 37 °C with shaking (100 rpm). After the incubation, 2 ml of the samples was centrifuged for 10 min at 25,000 RCF to eliminate the poor reliability originating from the creamed SLN aggregates and impurities (proteins present in pancreatic lipase and bile extract) in subsequent measurements, and the size and ZP of SLNs in the supernatant were measured using the Zetasizer.

2.8. Monitoring the lipolysis of solid lipid nanoparticles in vitro in simulated small intestinal fluid

The digestion of SLNs in the small intestine was assessed by profiling the particle lipolysis in a simulated small intestinal fluid.

The lipolysis pattern of SLNs was monitored for 2 h at 37 °C using the previously introduced titration method with slight modifications (Li & McClements, 2014). The simulated fluid was prepared by dissolving sodium chloride, calcium chloride, bile extract and pancreatic lipase in a 10 mM sodium phosphate buffer (pH = 7) at concentrations of 43.83, 11.098, 100, and 12 mg ml^{-1} , respectively, which was kept at 37 °C prior to the monitoring and adjusted to a pH of 7 using 1 M NaOH solution as necessary. Prior to titrations, all SLNs were diluted 10-fold with 10 mM sodium phosphate buffer (pH = 7), which was maintained at 37 °C and adjusted to a pH of 7 using 0.1 M NaOH solution as necessary. Finally, on the basis of the lipase-induced hydrolysis of one triacylglycerol (TAG) into one monoacylglycerol (MAG) and two free fatty acids (FFAs), the hydrolysis of the SLN samples (20 ml) was monitored by measuring the FFA released from the samples after the addition of the simulated small intestinal fluid (5 ml). The released amount of FFAs was quantified by adding 0.050 M NaOH solution to the reaction vessel to maintain the pH at 7 using an automatic titration unit (842 Titrando, Metrohm AG, Herisau, Switzerland), and the amount was converted into a % FFA value using the following equation:

$$\% \text{ FFA} = 100 \times (V_{\text{NaOH}} \times m_{\text{NaOH}} \times M_{\text{TS}}) / (w_{\text{TS}} \times 2),$$

where V_{NaOH} is the volume (ml) of the NaOH solution required to neutralize the produced FFAs, m_{NaOH} is the molarity (M) of the NaOH solution, M_{TS} is the molecular weight (891.45 g mol^{-1}) of the TS and w_{TS} is the total weight (0.1 g) of TS initially present in the reaction vessel. Blank experiments were also conducted without the enzyme to eliminate any pH decrease due to other factors.

2.9. Statistical analysis

Statistical analyses were conducted using Student's *t*-test with the SPSS Statistics version 23.0 software (IBM Co., Armonk, NY, USA). Data represent means of at least three independent experiments or measurements. The results were reported as averages and standard deviations of these measurements.

3. Results and discussion

3.1. Physicochemical characteristics of solid lipid nanoparticles

In general, the emulsifier, as an amphiphilic molecule, is comprised of two groups, which are the hydrophilic (head) and hydrophobic (tail) groups. The head and tail of each emulsifier used in this study were chosen with regards to changes in the molecular weight and structure. As shown in Table S2 (Supplementary Material), the heads were PEG polymer chains in which ethylene glycols repeated from 10 to 100 times and the tails were fatty acids (stearic acids) and fatty alcohols (lauryl, stearyl, or oleyl alcohol). In other words, the emulsifiers used in the present study were PEGylated emulsifiers, in which PEG polymer chains are covalently attached to the tails. The appearance of SLN systems prepared with the PEGylated emulsifiers is shown in Fig. S2 (Supplementary Material). According to the appearance after the dilution, at the same concentration of PEGylated emulsifiers, SLNs stabilized using PEG100S, PEG100SE and PEG20SS were more stable than those stabilized using PEG10S, PEG10SE, PEG10OE and PEG10LE, indicating that the larger PEG chains in the emulsifiers could enhance the colloidal stability of the SLNs. The creamed or sedimentary aggregations of SLNs were observed in the samples PEGylated using 10 ethylene glycols (PEG10S, PEG10OE and PEG10LE), except a PEG10SE-SLN sample. However, even in the samples stabilized using PEG10S, PEG10OE and PEG10LE, the concentration of the emulsifiers increased with the increase in the stability of the SLNs.

This result suggests that the use of large concentration or large PEG chain of the emulsifiers might improve the colloidal stability of SLNs.

The yield (%) value indicates the quantity of submicron lipid particles in a total SLN dispersion system without partial coalescence (Vanapalli & Coupland, 2001) and aggregation (Helgason, Awad, Kristbergsson, McClements, & Weiss, 2009). In this regard, the apparent colloidal stability shown in Fig. S2 can be converted to a numerical value using the yield (%) in Table 1. Of course, the yields (%) of all samples were increased with an increase in the emulsifier concentration because more emulsifiers can better stabilize the interface of the SLNs. Similar to the apparent results in Fig. S2, SLN samples prepared using PEG100S, PEG100SE and PEG20SS had larger values than those of SLN samples prepared using PEG10S, PEG10SE, PEG10OE and PEG10LE. Among PEGylated samples using 10 ethylene glycols, PEG10SE-SLNs peculiarly had the largest yield (%), which was close to the values of PEG100S, PEG100SE and PEG20SS samples at the same emulsifier concentration, and the reason for this peculiarity would need to be further verified.

The particle sizes (PSS) of all of the SLNs were reduced with increasing emulsifier concentrations (Table 1), which is attributed to the emulsifier's capability for holding the surface tension increased with a reduction in the droplet size during the manufac-

turing process (Aveyard, Binks, & Clint, 2003). On the other hand, the ZPs of all of the SLNs were elevated with increased emulsifier concentration due to the negative ZP values of all of the SLN samples (Table 1), which might be attributed to the presence of free fatty acids or other impurities remaining from TS production (McClements & Xiao, 2012). This result indicates that more PEGylated emulsifiers can increasingly bury sterically the negative charges on the surfaces of SLNs due to the electrostatic neutrality of PEG chains. SLNs emulsified using PEG10S and PEG100S had lower ZP values than PEG10SE- and PEG100SE-SLNs despite their PEG chains having the same molecular weight, which would be due to the double-bonded oxygen atom in a carbonyl group (C=O) of PEG10S and PEG100S. Meanwhile, PEG10SE-, PEG10OE-, and PEG10LE-SLNs had similar ZP values. These results in terms of the physicochemical stability of SLN samples would correlate with the PEGylated emulsifier covering on the SLN surface, and this is further discussed in the following section.

3.2. Emulsifier covering on the surface of solid lipid nanoparticles

In many previous studies, the Γ_s value was generally expressed as the mass per unit area (mg m^{-2}). However, in this research, to examine emulsifiers covering the SLN surface on a molecular level, the unit of the Γ_s was expressed as the number of emulsifiers per

Table 1
Physicochemical characteristics (yield, particle size, and ζ -potential) and surface load values of solid lipid nanoparticles emulsified by PEGylated emulsifiers.

Code name	Emulsifier concentration (mM)	Yield (%)	Particle size (nm)	ζ potential (mV)	Surface load (Γ_s) (nm^{-2}) ^a	$1/\Gamma_s$ (nm^2) ^b	$\sqrt{1/\Gamma_s}$ (nm) ^c
PEG10S	5.331	9.70	250.93 ± 3.02	−25.33 ± 1.11	0.72	1.38	1.17
	17.058	11.57	223.43 ± 3.34	−23.27 ± 0.67	2.13	0.47	0.69
	25.588	16.08	202.30 ± 1.71	−21.77 ± 0.71	2.88	0.35	0.59
	34.117	29.06	181.90 ± 0.66	−19.90 ± 1.06	3.45	0.29	0.54
	46.910	40.47	162.67 ± 1.98	−19.77 ± 0.50	3.41	0.29	0.54
PEG100S	5.331	86.93	264.77 ± 3.80	−16.13 ± 1.08	0.75	1.34	1.16
	17.058	94.65	204.07 ± 2.12	−16.07 ± 0.51	1.57	0.64	0.80
	25.588	94.54	176.77 ± 0.98	−12.37 ± 0.21	2.00	0.50	0.71
	34.117	95.73	167.17 ± 1.31	−11.03 ± 0.15	2.61	0.38	0.62
	46.910	95.71	120.67 ± 2.42	−8.89 ± 0.08	2.82	0.35	0.60
PEG10SE	5.331	60.49	391.93 ± 14.57	−19.83 ± 0.74	1.08	0.92	0.96
	17.058	85.71	273.53 ± 4.44	−13.13 ± 0.12	2.67	0.38	0.61
	25.588	90.77	216.20 ± 1.80	−9.07 ± 0.06	3.22	0.31	0.56
	34.117	91.76	176.00 ± 1.91	−8.97 ± 0.23	3.51	0.29	0.53
	46.910	95.30	100.38 ± 2.16	−7.37 ± 1.20	3.32	0.30	0.55
PEG100SE	5.331	92.81	333.73 ± 3.88	−6.00 ± 1.01	0.76	1.31	1.15
	17.058	93.16	227.20 ± 1.64	−2.54 ± 0.62	1.62	0.61	0.78
	25.588	94.78	225.23 ± 0.15	−2.97 ± 0.14	2.70	0.37	0.61
	34.117	93.82	172.33 ± 1.24	−1.77 ± 0.48	2.92	0.34	0.59
	46.910	96.22	122.67 ± 1.29	−0.35 ± 0.39	2.97	0.34	0.58
PEG10OE	5.331	9.69	180.00 ± 25.56	−18.60 ± 0.40	0.58	1.73	1.32
	17.058	18.55	126.40 ± 1.32	−16.20 ± 0.36	0.78	1.28	1.13
	25.588	25.50	119.77 ± 2.54	−15.47 ± 1.92	1.32	0.76	0.87
	34.117	36.25	96.11 ± 0.81	−12.90 ± 0.92	1.55	0.65	0.80
	46.910	74.55	92.77 ± 2.15	−6.11 ± 0.30	2.17	0.46	0.68
	65.000	96.63	79.65 ± 2.33	−5.49 ± 0.79	2.96	0.34	0.58
	75.000	95.85	70.47 ± 2.00	−1.39 ± 0.50	3.04	0.33	0.57
PEG10LE	5.331	14.58	205.40 ± 4.48	−21.83 ± 0.50	0.60	1.68	1.30
	17.058	33.57	129.80 ± 2.41	−19.27 ± 0.57	1.23	0.81	0.90
	25.588	48.66	115.87 ± 1.59	−14.37 ± 1.18	1.67	0.60	0.77
	34.117	54.87	91.03 ± 0.91	−12.00 ± 1.18	1.75	0.57	0.76
	46.910	60.54	86.56 ± 1.11	−8.50 ± 0.48	2.30	0.43	0.66
	65.000	77.50	83.63 ± 1.12	−6.05 ± 0.41	3.03	0.33	0.57
	75.000	89.14	72.93 ± 2.30	−5.15 ± 0.23	3.12	0.32	0.57
PEG20SS	5.331	76.34	280.30 ± 7.19	−16.83 ± 0.60	0.82	1.22	1.11
	17.058	93.59	217.93 ± 0.91	−14.13 ± 0.23	2.06	0.49	0.70
	25.588	93.56	196.27 ± 4.37	−13.93 ± 0.38	2.79	0.36	0.60
	34.117	95.94	151.67 ± 3.59	−12.40 ± 0.30	2.88	0.35	0.59
	46.910	95.61	114.37 ± 1.44	−12.03 ± 0.21	2.93	0.34	0.58

^a The number of emulsifiers adsorbing on the surface unit (1 nm^2) of the tristearin matrix.

^b Area occupied by an emulsifier adsorbing on the surface of the tristearin matrix.

^c The distance between the nearest emulsifiers.

$\text{nm}^2 (\text{nm}^{-2})$ by applying Avogadro's number and the molecular weight of each emulsifier. In this regard, the converted Γ_s values of SLN samples were determined as observed in Table 1. According to this result, in all PEGylated emulsifiers, the Γ_s was increased with increasing the emulsifier concentration below a certain level and then maintained at a relatively constant level. This phenomenon could indicate the saturation of the PEGylated emulsifier covering on the SLN surface. Surprisingly, all the saturation levels of the samples were approximately 3 nm^{-2} . The PEGylated emulsifiers comprised of a saturated chain of 18 carbons (PEG10S, PEG100S, PEG10SE, PEG100SE and PEG20SS) saturated the SLN surface at a concentration over 34.117 mM. However, the PEGylated emulsifier comprised of either an unsaturated chain of 18 carbons (PEG10OE) or a saturated chain of 12 carbons (PEG10LE) saturated the SLN surface at the concentration over 65.000 mM. This result indicated that a tail group in the PEGylated emulsifier molecule would determine the minimum concentration of the emulsifier for the saturation on the SLN surface.

The Γ_s values in Table 1 were converted into their reciprocal versions ($1/\Gamma_s$), indicating the area occupied by a single emulsifier molecule. In an assumption of the square arrival of emulsifiers on the SLN surface, the distance between the nearest emulsifiers was calculated as $\sqrt{1/\Gamma_s}$ ($>0.5 \text{ nm}$) using the square root of the area value in $1/\Gamma_s$. These results will be discussed more in depth in the following sections for examining the effect of the incubation conditions as well as the *in vitro* digestion of SLNs to assume the colloidal stability of the SLNs and molecular-level interfacial interactions among the TS, emulsifier, BA, pancreatic lipase and colipase during the small intestinal digestion process of the SLNs.

3.3. Effects of incubation conditions on the colloidal stability of solid lipid nanoparticles

A colloidal system including SLNs is usually influenced by the conditions of its dispersion medium. In particular, for the gastrointestinal digestion process of orally administered colloids, the pH and ion strength principally affect the aggregation of the colloidal system. In this respect, to assess the colloidal stability, SLNs were incubated in high ionic strength (containing various highly concentrated salts, e.g., NaHCO_3 , NaCl , KCl , CaCl_2 , etc.) and $\text{pH} = 3$ conditions for 2 h, and their PS and ZP values were measured as shown in Figs. 1 and 2, respectively. For the SLN samples prepared with 5.331 mM emulsifiers comprised of 10 ethylene glycols (PEG10-; i.e., PEG10S, PEG10SE, PEG10OE and PEG10LE), the PS values increased at both $\text{pH} = 3$ and high ionic strength conditions, indicating the aggregation of SLNs. Actually, for these samples after the incubation, the creamed aggregates of SLNs were large enough to be identified with the naked eye. However, there was no aggregation in PEG100- and PEG20-SLN samples. According to the ZP results in Fig. 2, the surface charge of all SLNs under $\text{pH} = 3$ and the high ionic strength conditions was almost zero. This suggested that even a low content of emulsifiers having ≥ 20 ethylene glycols could effectively prevent SLN aggregation due to their steric hindrance effect. Moreover, even in samples using PEG10-emulsifiers, the heavy aggregation of SLNs using emulsifiers over 17.058 mM was not observed, which could be attributed to the growth of the Γ_s . Therefore, increases of both the PEG molecular weight and the Γ_s can successfully improve the colloidal stability of SLNs under the acidic and high ionic strength conditions, such as in gastric fluid.

3.4. Physicochemical characteristics of solid lipid nanoparticles in the small intestine

The small intestine, particularly the duodenum, unlike the mouth and stomach, serves as an environment to hydrolyze most

of the orally administered lipids by the secretion of pancreatic lipase, colipase and bile salt (Larsen, Sassene, & Müllertz, 2011; Whitcomb & Lowe, 2007). Pancreatic lipase hydrolyzes a TAG to a MAG and two FFAs, and colipase, as a cofactor of pancreatic lipase, forms a complex with pancreatic lipase and helps the lipase to adsorb to the lipid surface (Lowe, 2002). BA, as a bio-surfactant, eliminates alien substances (such as proteins and emulsifiers) from the lipid surface to prepare the naked lipid surface where it can be adsorbed by the lipase (Maldonado-Valderrama et al., 2011).

To understand whether the lipases and BAs can adsorb to the surfaces of SLNs or not, the PS and ZP changes of the SLNs were monitored under a lipase solution and a bile solution, and Figs. 3 and 4 are the data for the PS and ZP values, respectively. The PS and ZP values of the SLN samples were slightly changed except for the PEG100S- and PEG100SE-SLN samples, but all SLNs were unhydrolyzed in the pancreatic lipase solution. Moreover, SLN creamed aggregates were observed in all SLN samples except the PEG100S- and PEG100SE-SLN samples as seen in Fig. S3 (Supplementary Material). Therefore, these results indicate the adherence of the lipase onto the small PEG chains (PEG10-) of emulsifier and the effective prevention of lipase adherence by the large PEG chains (PEG100-).

Bile extract used in this study was composed of 5 wt% phosphatidylcholine and 49 wt% BAs (10–15% glycodeoxycholic acid, 3–9% taurodeoxycholic acid, 0.5–7% deoxycholic acid, etc.) (Torcello-Gómez et al., 2011). Conventional surfactant molecules have a longitudinally widened structure called the hydrophilic head and hydrophobic tail, but BAs have a flat conformation (planar structure) composed of hydrophilic and hydrophobic faces (Maldonado-Valderrama et al., 2011). This flat conformation causes higher diffusivity on the lipid surface and lower surface pressure than the linear conformation of conventional emulsifiers (O'Connor, Ch'ng, & Wallace, 1983). In this manner, the adsorption of BAs onto the SLN interfaces covered by PEGylated emulsifiers is driven by competition for available interfacial area (Chu et al., 2009, 2010). On one hand, the larger PEG chains and their hydrogen bonding with water (hydration) will promote better interfacial packing of the PEG chains on SLNs and therefore better prevent the adsorption of BAs (Mannock, Harper, Gruner, & McElhaney, 2001). On the other hand, the hydration of PEG chains is considerably reduced with a slight increase in temperature from room temperature (25°C) to body temperature (37°C) (Mehnert & Mäder, 2001).

The PS values of all of the SLNs treated with bile extract were unchanged (i.e. non-aggregation) except for the SLNs using 5.331 mM emulsifiers (Fig. 3). However, the ZP values were significantly decreased after the bile extract treatment except for the SLN samples emulsified by PEG100S and PEG100SE over 17.058 mM (Fig. 4), which was attributed to the SLN interfacial adsorption of BAs and phospholipids in the bile extracts (ZP: $\sim -52 \text{ mV}$). Actually, according to the results for particle size distribution (Fig. S3), SLN creamed aggregates were observed in all SLN samples except the SLN samples prepared with PEG100S and PEG100SE at 46.910 mM. These results suggest that the 100 times repetition of ethylene glycols in the hydrophilic head of the SLN-stabilizing PEGylated emulsifiers is more effective than the 10 or 20 times repetition of ethylene glycols in preventing the water-TS interface from the adsorption of molecules in the treated bile extract, such as BAs, phospholipids, proteins, among others, despite the reduced hydration of PEG chains at 37°C .

3.5. Lipolysis of solid lipid nanoparticles in the small intestine

The percentage of FFAs generated from TS molecules in the SLNs (% FFA) was recorded as shown in Fig. 5. For SLN samples

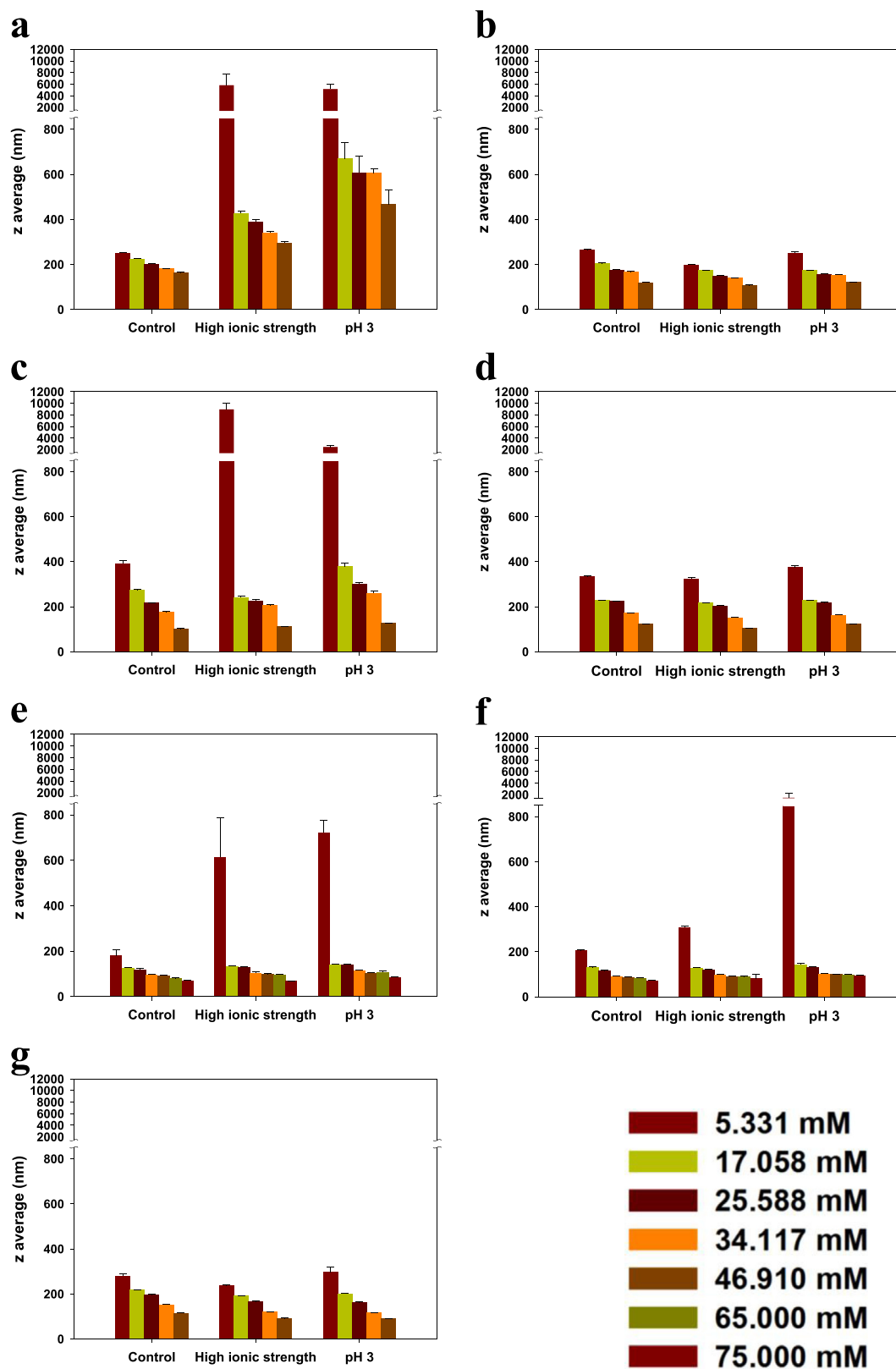


Fig. 1. Particle size (z average) of solid lipid nanoparticles emulsified by (a) PEG10S, (b) PEG100S, (c) PEG10SE, (d) PEG100SE, (e) PEG100E, (f) PEG10LE and (g) PEG20SS after incubation (2 h) in high ionic strength and acidic (pH = 3) conditions.

emulsified by PEG10SE (Fig. 5a), the hydrolysis rate was increased with increasing concentrations of PEG10SE. However, in SLNs stabilized by PEG100SE (Fig. 5b), the increase of the SLN hydrolysis rate was not observed, but the extent of FFA released became small-

er with an increase of the emulsifier concentration, which might be attributed to the action of a large PEG chain in PEG100SE in delaying the emulsifier displacement by BAs. Therefore, these results imply that the hydrolysis rate and extent of the SLNs could

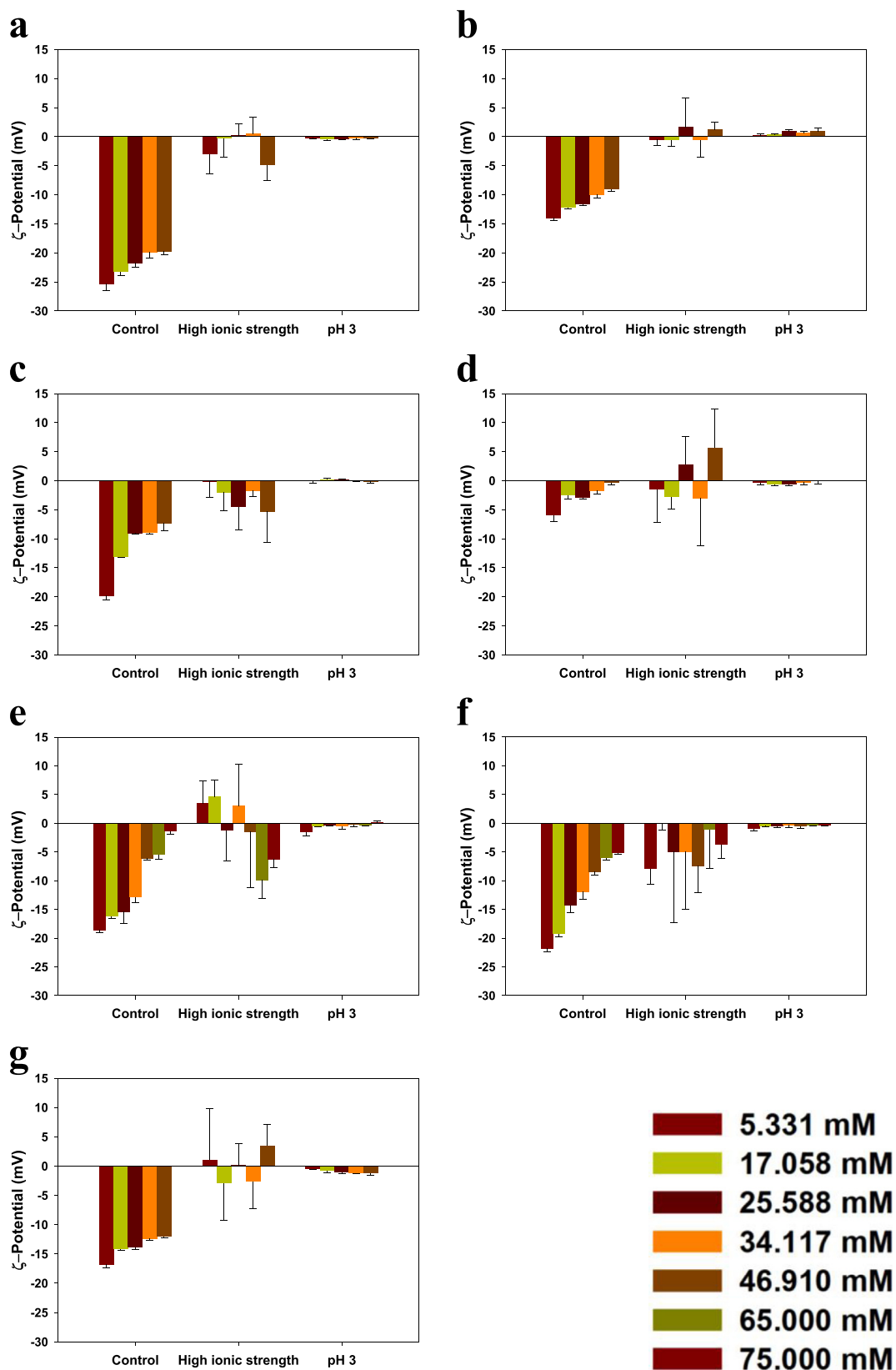


Fig. 2. ζ -potential of solid lipid nanoparticles emulsified by (a) PEG10S, (b) PEG100S, (c) PEG10SE, (d) PEG100SE, (e) PEG100E, (f) PEG10LE and (g) PEG20SS after incubation (2 h) in high ionic strength and acidic (pH = 3) conditions.

be controlled by the molecular weight/concentration of PEGylated emulsifiers, while full prevention of the BA/lipase-induced lipolysis of SLNs is impossible.

To more accurately capture PEGylated emulsifier-mediated changes to both the initial rate of lipolysis and the extent of digestion, the degree of digestion inhibition was expressed as the area

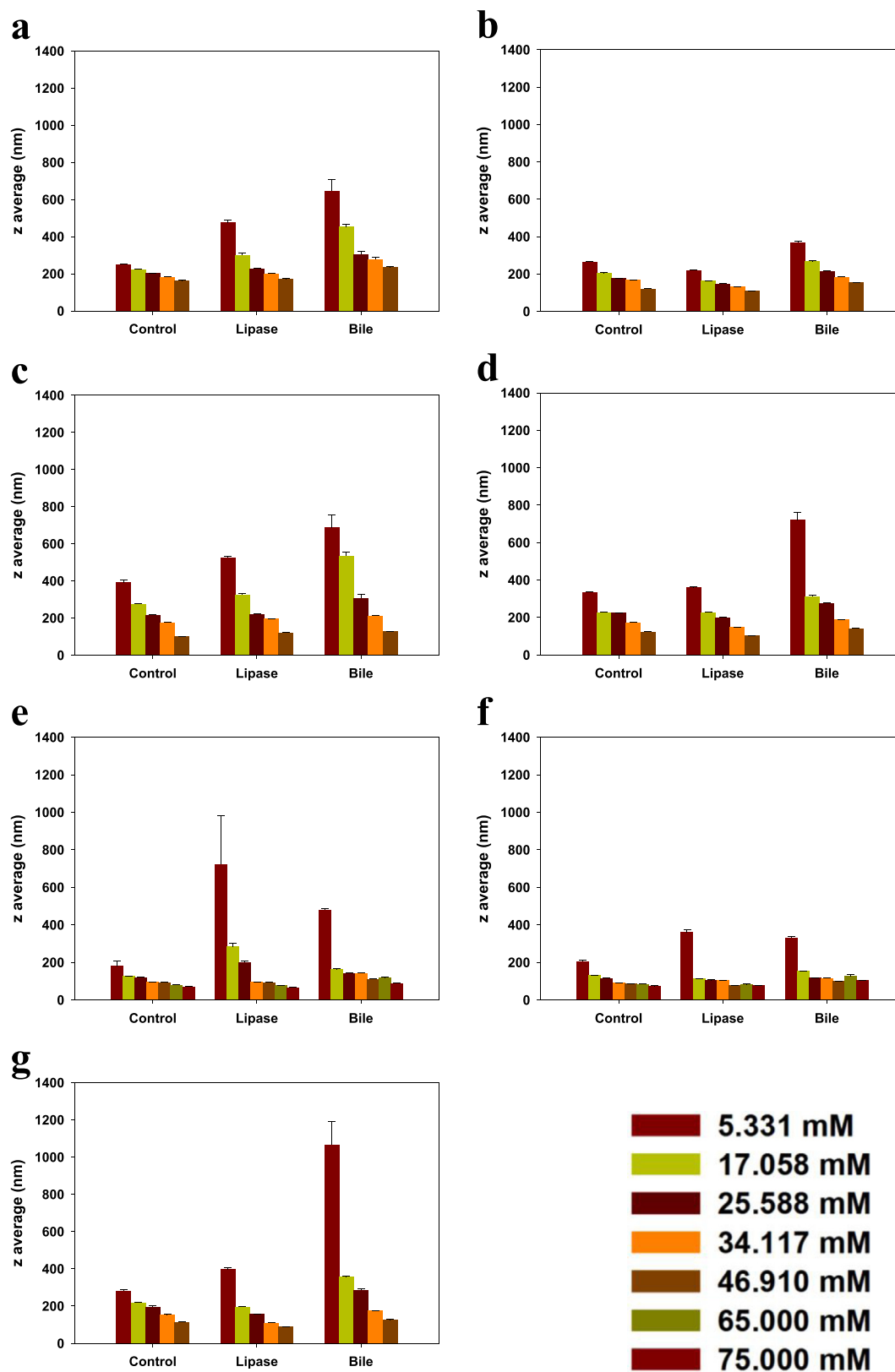


Fig. 3. Particle size (z average) of solid lipid nanoparticles emulsified by (a) PEG10S, (b) PEG100S, (c) PEG10SE, (d) PEG100SE, (e) PEG100E, (f) PEG10LE and (g) PEG20SS after treatment (2 h) with pancreatic lipase and bile extract solution.

under the % FFA curve ($AUC_{120\text{ min}}$) in a unit of % min. The $AUC_{120\text{ min}}$ for the PEG10SE samples was significantly enlarged as the concentration of PEG10SE used increased (Fig. 5c). On the other hand, the

$AUC_{120\text{ min}}$ for PEG100SE appeared to decrease with an increase in the concentration of PEG100SE. In common enzyme kinetics, a decrease in the size of the substrate causes an elevation of the

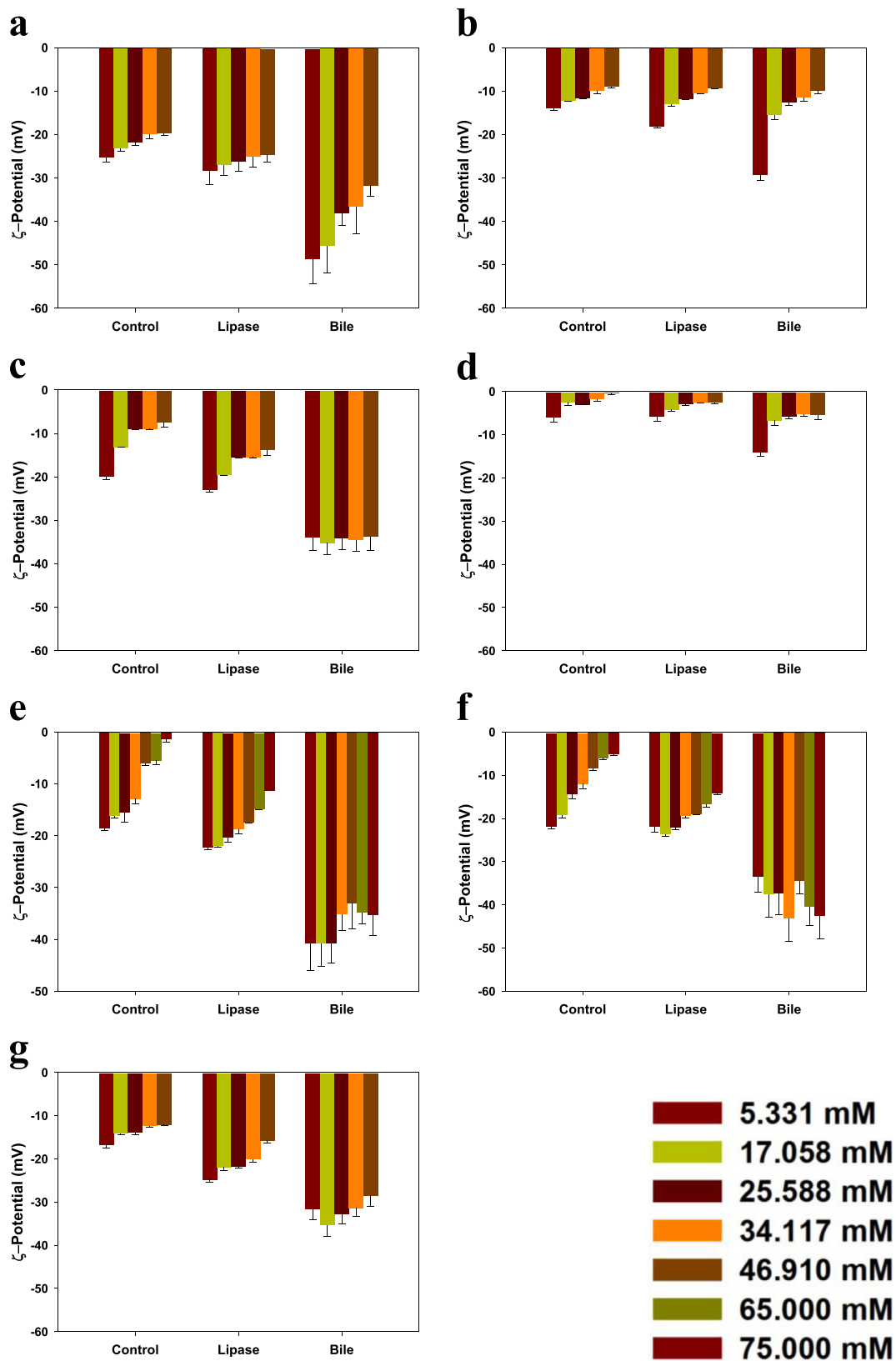


Fig. 4. ζ -potential of solid lipid nanoparticles emulsified by (a) PEG10S, (b) PEG100S, (c) PEG10SE, (d) PEG100SE, (e) PEG10OE, (f) PEG10LE and (g) PEG20SS after treatment (2 h) with pancreatic lipase and bile extract solution.

enzymatic reaction rate due to an increase of the reactive specific surface area of the substrate. In this regard, PEG10SE samples showed good agreement while PEG100SE samples did not (Fig. 5c).

Therefore, the PEG10SE at the interface cannot effectively inhibit the hydrolysis of the TS matrix by the action of the lipases and bile extract, but the PEG100SE shows enough inhibition to delay the

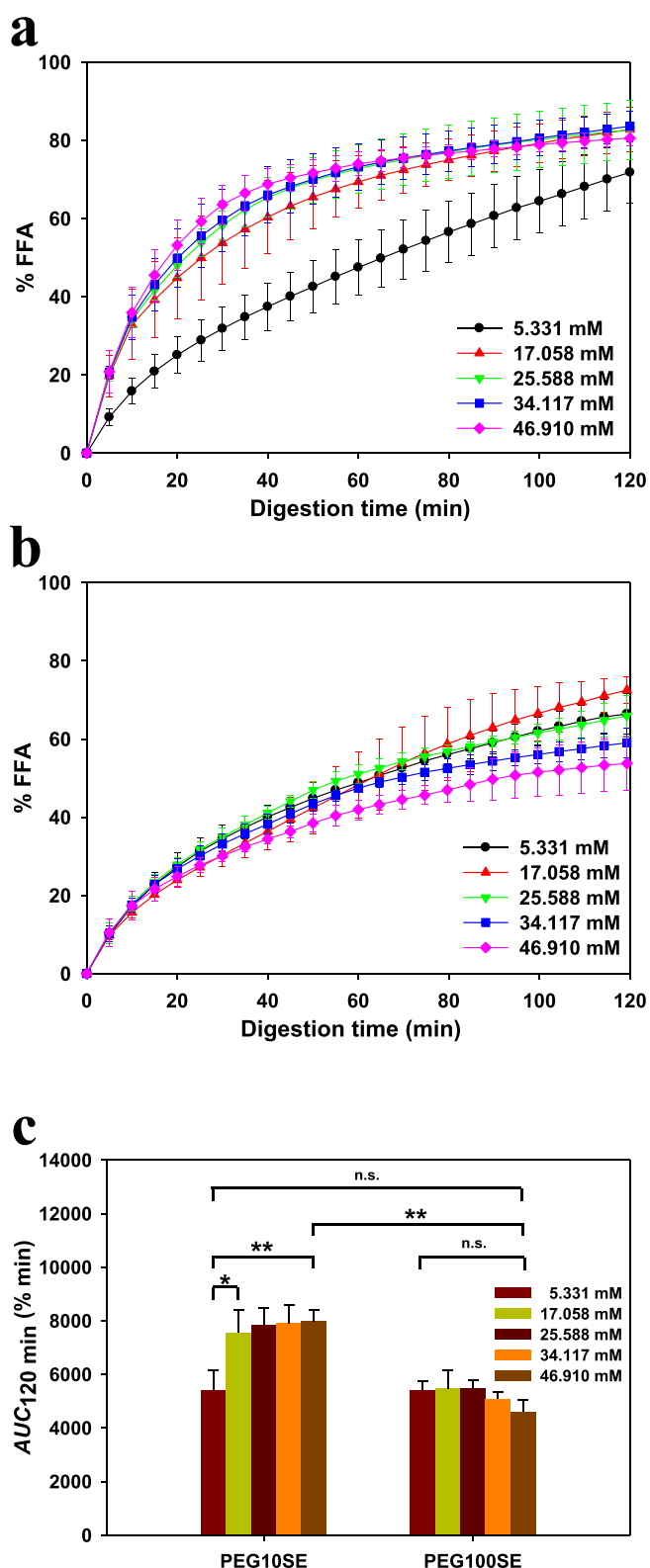


Fig. 5. Curves for the percentage of released free fatty acids (% FFA) from solid lipid nanoparticles emulsified by (a) PEG10SE and (b) PEG100SE in the simulated small intestine conditions as the emulsifier concentration changes and (c) area under the curves (AUC_{120min}) in the conditions for 120 min (n.s., non-significant; *, $p < 0.05$; and **, $p < 0.01$).

hydrolysis. The difference in the degree of digestion inhibition, resulting from the difference in the molecular weight of the PEG chain for various PEGylated surfactants, was previously reported

by Feeney, Williams, Pouton, and Porter (2014). Following their data, PEG10SE was even more effective than PEG100SE in inhibiting the lipolysis of lipid droplets, which would be the diametrical opposite of our result. This difference might be due to the different lipid matrices used (TS and the medium-chain triglyceride), which would need to be examined in further studies.

Colipase, as a cofactor of pancreatic lipase (~50,000 kDa), is an amphiphilic wedge-shaped protein with three fingers having hydrophobic tips (Egloff et al., 1995; Müller et al., 1996). It becomes a complex with the lipase and anchors the lipase onto the TAG surface (Sugar, Mizuno, Momsen, & Brockman, 2001). According previous studies, colipase binds to the non-catalytic C-terminal domain of the lipase, and the hydrophobic tips adhere to a lipid-water interface and help to bring the catalytic N-terminal domain of the lipase into close contact with the interface (Egloff et al., 1995; van Tilbeurgh et al., 1993). In addition, colipase requires approximately 1.45–5.00 nm² of hydrophobic area for adsorption, and the colipase/lipase complex requires approximately 9.00 nm² (≤ 1.8 nm by ≥ 5.0 nm) to form a lipid-water interface binding site (Sugar et al., 2001). Therefore, it is impossible that the lipase or lipase/colipase complex adsorbs onto the SLN surface alone and hydrolyzes TS molecules of SLNs without the help of BAs. As a result, the digestion of SLNs in the environment of the small intestine should be governed by the adsorption of BAs onto the interface.

As mentioned previously, BA has a peculiar planar amphiphilic structure, which brings higher affinity with the TS surface of SLNs when compared with the PEGylated emulsifiers used in the present study. Despite the high affinity, BAs also require a minimum hydrophobic area to adsorb onto the SLN surface. Cholic acid, as the representative of BAs, has the bottom dimensions (hydrophobic face) of 2.6 nm² and a height of 0.8 nm (Despa, Luo, Li, Duan, & Lam, 2010). With only taking into account the dimensions of cholic acid and the $1/\Gamma_s$ values (Table 1), BAs cannot adsorb on the TS surface of all of the SLN samples because of the $1/\Gamma_s$ values < 2.6 nm². However, only PEG100-samples (PEG100S and PEG100SE) using ≥ 17.058 mM can inhibit the adsorption of BAs onto the SLN surface according to the ZP results in Fig. 4, resulting from the BA adsorption driven by competition with PEGylated emulsifiers. Additionally, lipolysis was even observed in all of the PEG100-samples. This result suggests that the PEGylated emulsifier cannot thoroughly prevent BA adsorption and lipolysis, but it can delay the competitive adsorption of BAs and lipolysis.

After considering all of the factors, such as sizes of TS, emulsifiers, BAs, colipase and lipase, the digestion mechanism of SLNs covered with PEGylated emulsifiers was suggested as displayed in the pictorial diagrams in Fig. S4 (Supplementary Material). SLNs with low Γ_s of emulsifiers containing a small PEG chain (PEG10S, PEG10SE, PEG10OE, PEG10LE and PEG20SS) are digested rapidly due the ease of BA adsorption onto the TS surface. SLNs with high Γ_s of the small-chained emulsifiers are also digested in a relatively short time because of the fast displacement of the emulsifiers by BAs. Thus, the digestion rates of SLN samples covered by the small-chained emulsifiers could mainly depend on their PS. In contrast, SLNs stabilized by the large-chained emulsifiers (PEG100S and PEG100SE) are hydrolyzed slowly due to the hindrance effect by the PEG chain. This effect of the large emulsifiers is in a good accordance with previously reported literature data, e.g., the effects of digalactosyldiacylglycerol (Chu et al., 2010), Poloxamer 188 (Müller et al., 1996) and Poloxamer 407 (Olbrich & Müller, 1999).

4. Conclusions

In this study, the colloidal stabilities and GIT digestions of TS nanoparticles stabilized with various PEGylated emulsifiers were

examined at the molecular level. Particularly, the SLN lipolysis induced by the action of bile salts, colipase, and pancreatic lipase in the small intestinal tract was minutely studied *in vitro* under the simulated conditions. According to the results, the SLNs coated with small-chained PEGylated emulsifiers were more significantly hydrolyzed than those covered with large-chained PEGylated emulsifiers. Additionally, the PS reduction increased the degree of digestion (AUC_{120min}) of the SLNs coated with small-chained PEGylated emulsifiers. On the other hand, the Γ_s reduction, rather than the PS reduction, increased the AUC_{120min} of the SLNs coated with large-chained PEGylated emulsifiers. This result suggests that the large-chained PEGylated emulsifiers can hinder more the adsorption of BAs, colipase, and pancreatic lipase than the small-chained PEGylated emulsifiers. Consequently, we demonstrated that the digestion fate of the orally administered SLNs could be controlled by rational design in terms of choosing the type and concentration of PEGylated emulsifiers. In conclusion, this research could serve as a basis for further studies to develop an oral lipid carrier system for functional foods or drugs.

Acknowledgements

This research was supported by the Basic Science Research Program through the National Research Foundation of Korea (NRF) funded by the Ministry of Science, ICT and Future Planning (NRF-2016R1D1A1B03936106).

Appendix A. Supplementary data

Supplementary data associated with this article can be found, in the online version, at <http://dx.doi.org/10.1016/j.foodchem.2017.06.137>.

References

- Aveyard, R., Binks, B. P., & Clint, J. H. (2003). Emulsions stabilised solely by colloidal particles. *Advances in Colloid and Interface Science*, 100, 503–546.
- Ban, C., Lim, S., Chang, P., & Choi, Y. J. (2014). Enhancing the stability of lipid nanoparticle systems by sonication during the cooling step and controlling the liquid oil content. *Journal of Agricultural and Food Chemistry*, 62(47), 11557–11567.
- Chu, B., Gunning, A. P., Rich, G. T., Ridout, M. J., Faulks, R. M., Wickham, M. S. J., ... Wilde, P. J. (2010). Adsorption of bile salts and pancreatic colipase and lipase onto digalactosyldiacylglycerol and dipalmitoylphosphatidylcholine monolayers. *Langmuir*, 26(12), 9782–9793.
- Chu, B., Rich, G. T., Ridout, M. J., Faulks, R. M., Wickham, M. S. J., & Wilde, P. J. (2009). Modulating pancreatic lipase activity with galactolipids: Effects of emulsion interfacial composition. *Langmuir*, 25(16), 9352–9360.
- Despa, F., Luo, J. T., Li, J., Duan, Y., & Lam, K. S. (2010). Cholic acid micelles—Controlling the size of the aqueous cavity by PEGylation. *Physical Chemistry Chemical Physics*, 12(7), 1589–1594.
- Egloff, M., Marguet, F., Buono, G., Verger, R., Cambillau, C., & van Tilbeurgh, H. (1995). The 2.46 Å resolution structure of the pancreatic lipase-colipase complex inhibited by a C11 alkyl phosphonate. *Biochemistry*, 34(9), 2751–2762.
- Feeney, O. M., Williams, H. D., Pouton, C. W., & Porter, C. J. H. (2014). 'Stealth' lipid-based formulations: Poly(ethylene glycol)-mediated digestion inhibition improves oral bioavailability of a model poorly water soluble drug. *Journal of Controlled Release*, 192, 219–227.
- Gref, R., Lück, M., Quellec, P., Marchand, M., Dellacherie, E., Harnisch, S., ... Müller, R. H. (2000). 'Stealth' corona-core nanoparticles surface modified by polyethylene glycol (PEG): Influences of the corona (PEG chain length and surface density) and of the core composition on phagocytic uptake and plasma protein adsorption. *Colloids and Surfaces B: Biointerfaces*, 18(3), 301–313.
- Helgason, T., Awad, T. S., Kristbergsson, K., McClements, D. J., & Weiss, J. (2009). Effect of surfactant surface coverage on formation of solid lipid nanoparticles (SLN). *Journal of Colloid and Interface Science*, 334(1), 75–81.
- Hur, S. J., Joo, S. T., Lim, B. O., Decker, E. A., & McClements, D. J. (2011). Impact of salt and lipid type on *in vitro* digestion of emulsified lipids. *Food Chemistry*, 126(4), 1559–1564.
- Jeong, J. H., Park, T. G., & Kim, S. H. (2011). Self-assembled and nanostructured siRNA delivery systems. *Pharmaceutical Research*, 28(9), 2072–2085.
- Khossravi, M., Kao, Y. H., Mrsny, R. J., & Sweeney, T. D. (2002). Analysis methods of polysorbate 20: A new method to assess the stability of polysorbate 20 and established methods that may overlook degraded polysorbate 20. *Pharmaceutical Research*, 19(5), 634–639.
- Kong, F., & Singh, R. P. (2008). Disintegration of solid foods in human stomach. *Journal of Food Science*, 73(5), R67–R80.
- Larsen, A. T., Sassene, P., & Müllertz, A. (2011). *In vitro* lipolysis models as a tool for the characterization of oral lipid and surfactant based drug delivery systems. *International Journal of Pharmaceutics*, 417(1), 245–255.
- Li, Y., & McClements, D. J. (2014). Modulating lipid droplet intestinal lipolysis by electrostatic complexation with anionic polysaccharides: Influence of cosurfactants. *Food Hydrocolloids*, 35, 367–374.
- Lowe, M. E. (2002). The triglyceride lipases of the pancreas. *The Journal of Lipid Research*, 43(12), 2007–2016.
- Maldonado-Valderrama, J., Gunning, A. P., Ridout, M. J., Wilde, P. J., & Morris, V. J. (2009). The effect of physiological conditions on the surface structure of proteins: Setting the scene for human digestion of emulsions. *The European Physical Journal E*, 30(2), 165–174.
- Maldonado-Valderrama, J., Gunning, A. P., Wilde, P. J., & Morris, V. J. (2010). *In vitro* gastric digestion of interfacial protein structures: Visualisation by AFM. *Soft Matter*, 6(19), 4908–4915.
- Maldonado-Valderrama, J., Wilde, P., Macierzanka, A., & Mackie, A. (2011). The role of bile salts in digestion. *Advances in Colloid and Interface Science*, 165(1), 36–46.
- Maldonado-Valderrama, J., Woodward, N. C., Gunning, A. P., Ridout, M. J., Husband, F. A., Mackie, A. R., ... Wilde, P. J. (2008). Interfacial characterization of β -lactoglobulin networks: Displacement by bile salts. *Langmuir*, 24(13), 6759–6767.
- Mannock, D. A., Harper, P. E., Gruner, S. M., & McElhaney, R. N. (2001). The physical properties of glycosyl diacylglycerols. Calorimetric, X-ray diffraction and Fourier transform spectroscopic studies of a homologous series of 1, 2-di-O-acyl-3-O-(β -D-galactopyranosyl)-sn-glycerols. *Chemistry and Physics of Lipids*, 111(2), 139–161.
- McClements, D. J. (2007). Critical review of techniques and methodologies for characterization of emulsion stability. *Critical Reviews in Food Science and Nutrition*, 47(7), 611–649.
- McClements, D. J., Decker, E. A., & Park, Y. (2008). Controlling lipid bioavailability through physicochemical and structural approaches. *Critical Reviews in Food Science and Nutrition*, 49(1), 48–67.
- McClements, D. J., & Xiao, H. (2012). Potential biological fate of ingested nanoemulsions: Influence of particle characteristics. *Food & Function*, 3(3), 202–220.
- Mehnert, W., & Mäder, K. (2001). Solid lipid nanoparticles: Production, characterization and applications. *Advanced Drug Delivery Reviews*, 47(2), 165–196.
- Müller, R. H., Mäder, K., & Gohla, S. (2000). Solid lipid nanoparticles (SLN) for controlled drug delivery—A review of the state of the art. *European Journal of Pharmaceutics and Biopharmaceutics*, 50(1), 161–177.
- Müller, R. H., Rühl, D., & Runge, S. A. (1996). Biodegradation of solid lipid nanoparticles as a function of lipase incubation time. *International Journal of Pharmaceutics*, 144(1), 115–121.
- Nagaoka, S., & Nakao, A. (1990). Clinical application of antithrombotic hydrogel with long poly (ethylene oxide) chains. *Biomaterials*, 11(2), 119–121.
- Niidome, T., Yamagata, M., Okamoto, Y., Akiyama, Y., Takahashi, H., Kawano, T., ... Niidome, Y. (2006). PEG-modified gold nanorods with a stealth character for *in vivo* applications. *Journal of Controlled Release*, 114(3), 343–347.
- O'Connor, C. J., Ch'ng, B. T., & Wallace, R. G. (1983). Studies in bile salt solutions: 1. Surface tension evidence for a stepwise aggregation model. *Journal of Colloid and Interface Science*, 95(2), 410–419.
- Olbrich, C., & Müller, R. H. (1999). Enzymatic degradation of SLN—Effect of surfactant and surfactant mixtures. *International Journal of Pharmaceutics*, 180(1), 31–39.
- Porter, C. J. H., Pouton, C. W., Cuine, J. F., & Charman, W. N. (2008). Enhancing intestinal drug solubilisation using lipid-based delivery systems. *Advanced Drug Delivery Reviews*, 60(6), 673–691.
- Sugar, I. P., Mizuno, N. K., Momen, M. M., & Brockman, H. L. (2001). Lipid lateral organization in fluid interfaces controls the rate of colipase association. *Biophysical Journal*, 81(6), 3387–3397.
- Torcello-Gómez, A., Maldonado-Valderrama, J., Martín-Rodríguez, A., & McClements, D. J. (2011). Physicochemical properties and digestibility of emulsified lipids in simulated intestinal fluids: Influence of interfacial characteristics. *Soft Matter*, 7(13), 6167–6177.
- van Tilbeurgh, H., Egloff, M., Martinez, C., Rugani, N., Verger, R., & Cambillau, C. (1993). Interfacial activation of the lipase-procolipase complex by mixed micelles revealed by X-ray crystallography. *Nature*, 362, 814–820.
- Vanapalli, S. A., & Coupland, J. N. (2001). Emulsions under shear—The formation and properties of partially coalesced lipid structures. *Food Hydrocolloids*, 15(4), 507–512.
- Whitcomb, D. C., & Lowe, M. E. (2007). Human pancreatic digestive enzymes. *Digestive Diseases and Sciences*, 52(1), 1–17.